Supporting Information for:

Plasmon Assisted $Ti_3C_2T_x$ Grafting and Surface Termination Tuning for Enhancement of Flakes Stability and Humidity Sensing Performance

Vladislav Buravets[a], Anastasiia Olshtrem[a], Vasilii Burtsev[a], Gorin Oleg[a], Sergii Chertopalov[b], Andrei Chumakov[c], Matthias Schwartzkopf[c], Jan Lancok[b], Vaclav Svorcik[a], Oleksiy Lyutakov[a], Elena Miliutina[a, *]

[a] *Department of Solid State Engineering, University of Chemistry and Technology, 16628 Prague, Czech Republic*

[b] *Institute of Physics of the Czech Academy of Sciences, Na Slovance 1999/2, 18200 Prague, Czech Republic*

[c] *Deutsches Elektronen-Synchrotron (DESY), 22607 Hamburg, Germany*

---

[*]Corresponding author: *miliutie@vscht.cz*

Experimental section

Synthesis of $Ti_3C_2T_x$ flake

The MILD method was used to synthesize $Ti_3C_2T_x$ (MXene) [S1]. Prior to selective etching of aluminium from Ti_3AlC_2 MAX phase, the MAX phase ceramics were crushed using an alumina mortar and pestle and then sieved to isolate particles with sizes less than 45 μm. The etchant was made by dissolving 300 mg of LiF (99.98 % metals basis, Alfa Aesar) in 6 ml of 6 M HCl in a 50 mL plastic tube. Next, 300 mg of the sieved MAX phase powder (with particle sizes below 45 μm) was added to the prepared etchant and stirred at 22 °C for 24 h. After the aluminium etching, MXene was washed multiple times until the pH of the supernatant reached value of 6. To delaminate MXene flakes, sample (15 mL DI water in a 50 mL plastic test tube) was manually shaken for 5 min followed by 30 min of centrifugation at 3500 rpm to separate the non-delaminated MXene.

Modification of $Ti_3C_2T_x$

4-carboxybenzenediazonium tosylate (ADT-COOH) and 4-Trifluoromethylbenzene Diazonium (ADT-CF_3) were prepared according to the published procedure [S2]. The 10 mL of MXene suspension (3 mg·mL^{-1}) was mixed with 3 mL of freshly prepared 3 mM alcohol-aqueous solution (methanol:water – 1:5) of ADT-COOH or ADT-CF_3 and then subjected to LED irradiation with 780 nm central emission wavelengths for 2 h. Flakes were subsequently washed using several repeated separation-redispersion cycles with distilled H_2O (2x) and methanol (2x).

Material characterization

Scanning electron microscopy (SEM) and energy-dispersive X-ray spectroscopy (EDX) (LYRA3 GMU, Tescan, CR) were collected at the operating voltage of 10 kV and a beam current of 600 pA. The samples were positioned at a 90° angle on a specialized table for the purpose of cross-section measurements.

Surface-Enhanced Raman Spectroscopy (SERS) spectra were measured using ProRaman-L spectrometer with 785 nm excitation wavelength and a laser power of 35 mW. Spectra were collected during 100 s.

X-ray diffraction (XRD) measurements were performed with the utilization of Empyrean, Malvern Panalytical device using Cu $K_{<\alpha>}$ radiation (*wavelength* = 1.5406, *U* = 45 kV, *I* = 30 mA). The incident angle was 0.85 ° corresponding to ∼10 mm of sample irradiation.

X-ray photoelectron spectroscopy (XPS) was performed using an Omicron Nanotechnology ESCAProbeP spectrometer fitted with a monochromatic Al K-alpha X-ray source at 1486.7 eV.

Quartz crystal microbalances (openQCM Q-1) and AT-cut quartz crystal (Novaetech S.r.l., Italy) with Ti/Au electrodes (10 MHz, diameter 14 mm) were used for mass change determination, performed at different humidity levels.

Water contact angles (CAs) were measured by Drop Shape Analyzer–DSA100 (Krüss, Germany) at 5 positions (drop volume—2 μL) at room temperature. All measurements were repeated on 10 randomly selected points.

UV–visible spectrophotometry (UV-Vis) absorption spectra of diazonium salts and delaminated MXene flakes were recorded using a Lambda 25 UV/Vis/NIR spectrometer (PerkinElmer) in a 300–1000 nm spectral range.

Fourier transform infrared (FTIR) spectra were measured on Nicolet iS5 Spectrometer. All FTIR measurements were collected in attenuated total reflection mode, in the 2600 to 4000 cm^{-1} spectral range with a resolution of 4 cm^{-1}. The obtained spectra were baseline-corrected (underlying background subtracted) to highlight the -OH group presence.

Stability tests. The estimation of the flakes and the sensor stability was performed in two modes: (i) – flakes storage under ambient conditions for 6 months, oxidation of flakes was subsequently estimated by XPS as a function of the surface grafting; (ii) - artificial aging (50 °C and 100% humidity level) with online estimation of the resistance of MXene films.

Preparation and testing of humidity sensor

The MXene films' response to humidity was evaluated within a custom-built chamber, with all experiments carried out at 24 °C. Humidity control within the chamber was achieved by passing dry air (∼0 % RH) through solutions with established humidity ($CaCl_2$ 7 %, $MgCl_2$ 33 %, K_2CO_3 43 %, NH_4NO_3 65 %, NaCl 75 %, KCl 82.4 %, K_2SO_4 97.3 %), while a commercial humidity sensor

(DHT22, Waveshare Electronics, China) was used to control the humidity level in the box. The current passed through MXene films was monitored using a Palm Sens 4 (Palm Instruments, Netherlands).

In situ GIWAXS measurements

The interlayer distance of MXene films was measured at controlled humidity levels using grazing-incidence wide-angle X-ray scattering (GIWAXS) at the P03 beamline of the PETRA III synchrotron [S3] (Deutsches Elektronen-Synchrotron DESY, Hamburg, Germany). A grazing incidence angle of 0.5 ° was chosen to maximize scattering intensity from the samples, and a standard calibration of sample-to-detector distance with silver behenate was performed prior to the GIWAXS experiment to provide uncertainty in absolute *d*-spacing of below 0.01 nm^{-1} for d-spacing of 10 nm^{-1}. The humidity level was controlled in a specially designed humidity cell [S4] with Kapton windows during the experiments, using a total flow of 1000 mL min^{-1} of mixed dry and wet nitrogen introduced to the cell with VEMD (Festo) flow controllers. The humidity level was monitored at the inlet and outlet of the experimental cell using KIP-20 temperature-humidity transducers based on HIH-4000 (Honeywell, accuracy 2 % RH) sensors. Additionally, diffraction patterns of wetted samples were obtained by placing a water drop onto the sample surface under >98 % humidity. The incident photon beam had an energy of 11.83 keV (λ = 1.048Å, $\Delta\lambda/\lambda < 3\cdot10^{-4}$) with a beam size of 27 × 22 μm^2, focused at the sample position by 2D compound refractive Be lenses. The scattered X-rays were captured using a LAMBDA 9M detector (X-Spectrum, pixel size 55×55 μm^2). The sample-to-detector distance was set to SDD=479 mm. GIWAXS data were analysed using the DPDAK (Directly Programmable Data Analysis Kit) software package [S5].

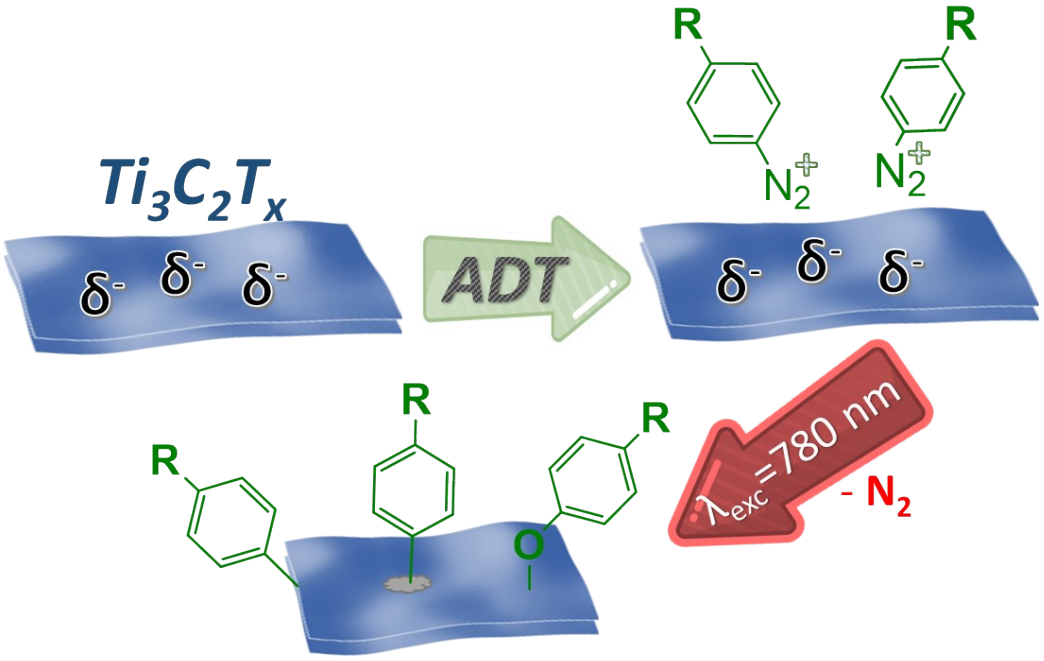

Fig. S1

Schematic representation of flakes grafting (electrostatic surface sorption of ADT molecules, plasmon-induced radicals formation, radicals grafting to MXene surface on edges, -OH terminals or defects).

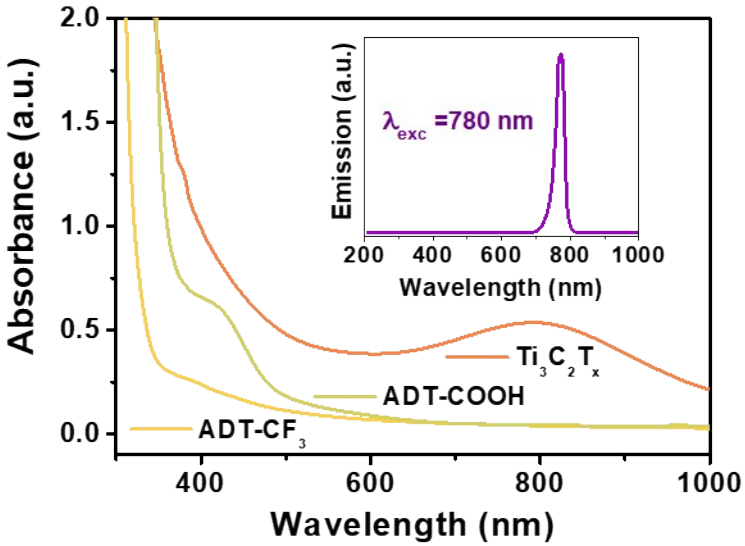

Fig. S2

UV–Vis spectra of MXene suspension and ADT salt solutions. The emission spectrum of used LED is given as insert (LED light can be absorbed by $Ti_3C_2T_x$ flakes, but not by ADTs molecules).

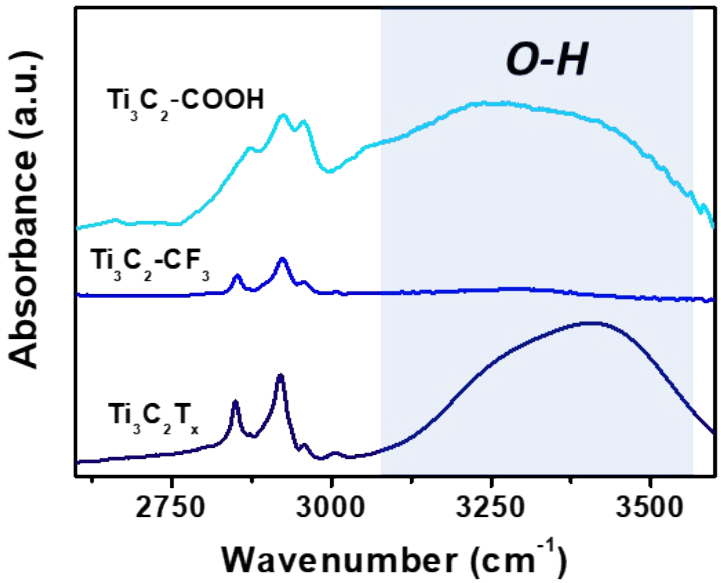

Fig. S3

Changes of characteristic "–OH" related region of FTIR spectrum as a function of flakes' surface termination – demonstration of grafting with formation of –O-C_6H_4-CF_3 bridges and disappearance of characteristic –OH vibration band.

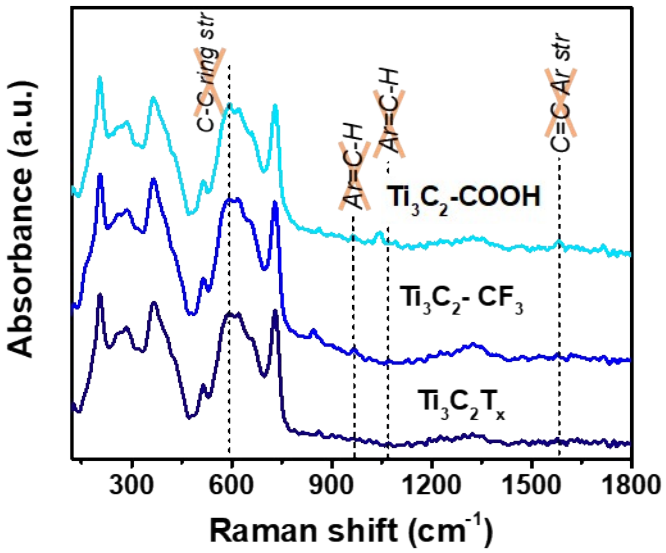

Fig. S4

SERS spectra of MXene powders after flakes interaction with ADT salts without plasmon triggering. The absence of characteristic SERS bands (dashed lines) and overall conservation of spectral patterns indicate the absence of surface termination tuning and highlight the key role of plasmon triggering in ADT activation and flakes surface grafting.

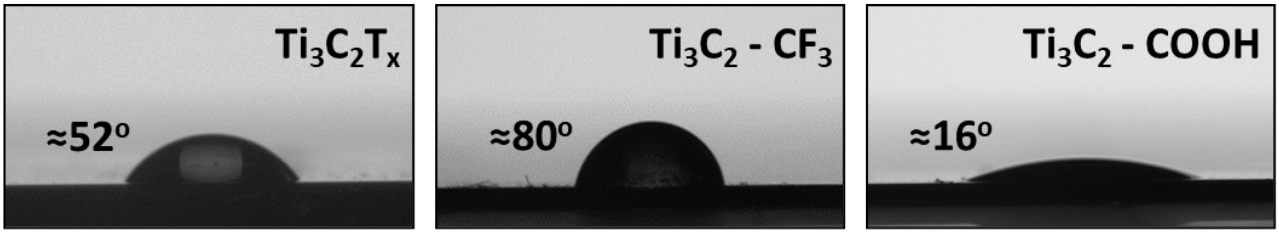

Fig. S5 Water contact angles were measured on the surface of $Ti_3C_2T_x$ films created from pristine and grafted flakes.

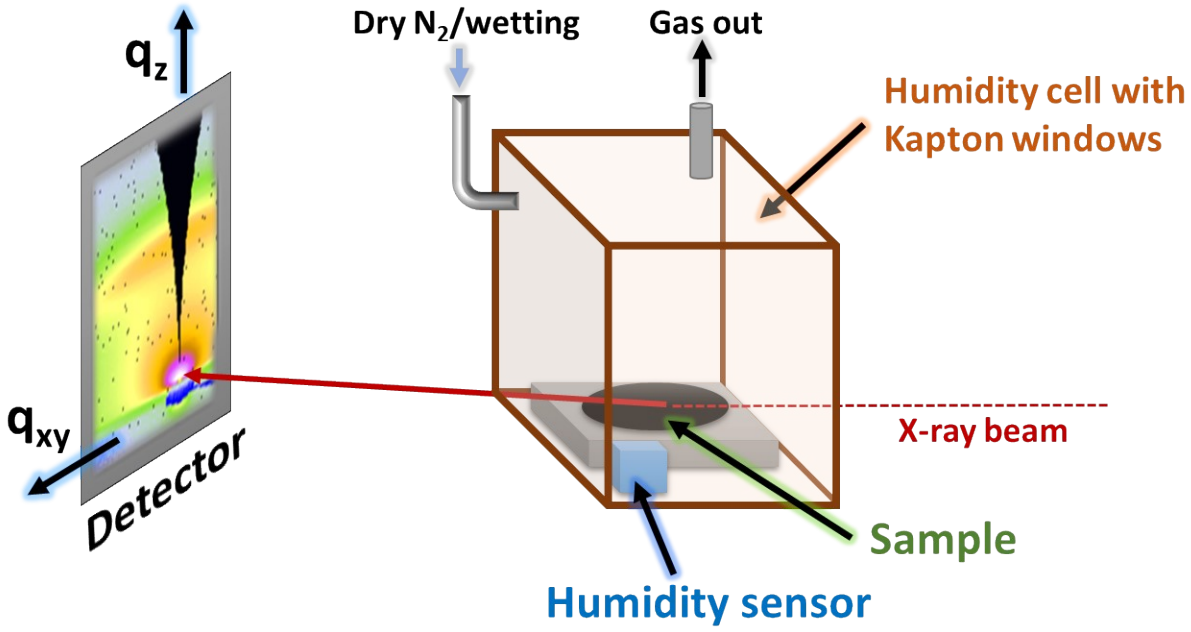

Fig. S6

Schematic representation of *in situ* GIWAXS measurements, performed is specially designed cell at different humidity levels.

Table S1

Affiliation of SERS bands, measured on the surface of pristine and grafted $Ti_3C_2T_x$ flakes.

Assignment	Peak Position, cm^{-1}
$Ti_3C_2T_x$	
Surface functional groups: O. OH, F and A_{1g} and E_g vibration modes	206, 260, 285, 364, 515, 618, 662, 731
Ti_3C_2-CF_3	
CF_3 rocking vib	163
Ring def	240
Sym CF_3 def vib	454
Ar=C-H out-of-plane str	665, 966
CF def vib	847
Ar=C-H in-plane str	1087
C=C Ar str	1580
Ti_3C_2-COOH	
Ring def	240
Ar=C-H out-of-plane str	665, 760, 966
O-H out-of-plane	859, 966
C-O str	1041
Ar=C-H in-plane str	1087
O-H in-plane str	1359
C=C Ar str	1580

References

[S1] Y. Dong, S. Chertopalov, K. Maleski, B. Anasori, L. Hu, S. Bhattacharya, A. M. Rao, Y. Gogotsi, V. N. Mochalin and R. Podila, *Adv. Mater.*, 2018, **30**, 1705714.

[S2] O. Guselnikova, P. Postnikov, R. Elashnikov, M. Trusova, Y. Kalachyova, M. Libansky, J. Barek, Z. Kolska, V. Švorčík and O. Lyutakov, *Colloid Surf. A-Physicochem. Eng. Asp.*, 2017, **516**, 274–285.

[S3] A. Buffet, A. Rothkirch, R. Döhrmann, V. Körstgens, M. M. Abul Kashem, J. Perlich, G. Herzog, M. Schwartzkopf, R. Gehrke, P. Müller-Buschbaum and S. V. Roth, *J Synchrotron Rad*, 2012, **19**, 647–653.

[S4] A. A. Eliseev, A. A. Poyarkov, E. A. Chernova, A. A. Eliseev, A. P. Chumakov, O. V. Konovalov and D. I. Petukhov, *2D Mater.*, 2019, **6**, 035039.

[S5] G. Benecke, W. Wagermaier, C. Li, M. Schwartzkopf, G. Flucke, R. Hoerth, I. Zizak, M. Burghammer, E. Metwalli, P. Müller-Buschbaum, M. Trebbin, S. Förster, O. Paris, S. V. Roth and P. Fratzl, *J Appl Cryst*, 2014, **47**, 1797–1803.